

Intelligent Wireless Remote Control System Design for a Biped Robot

Chih-Hsuan Chen¹, Chih-Min Lin^{1, 2,*}

¹Department of Electrical Engineering, Yuan Ze University, Taoyuan, Taiwan, ROC.

²School of Informatics, Xiamen University, Xiamen, Fujian, China.

Received 30 July 2017; received in revised form 15 August 2017; accepted 26 August 2017

Abstract

This paper presents the design and implementation of an intelligent wireless remote control system for a biped robot. A recurrent cerebellar model neural network (RCMNN) is introduced, then it is used for the walking control of a biped robot. Furthermore, the remote communication module is designed for the remote control of a robot. Finally, experimental results show that the developed system can achieve satisfactory control performance for the walking control of a high-order nonlinear biped robot.

Keywords: biped robot, wireless remote control, cerebellar model neural network

1. Introduction

Biped robots are a favorite topic in the field of robotics [1-3]. Many dynamics analysis and system control researches have been presented for the biped robots [4-5]. In order to achieve adaptive control of a biped robot to face unknown environment, an intelligent control algorithm will be proposed in this study.

Cerebellar model neural network (CMNN), first proposed by Albus, has been applied to control a robot manipulator [6]. CMNN has been applied for the control of complex dynamic systems due to its good generalizing capability and fast learning property. In this paper, a recurrent CMNN (RCMNN) is introduced; then, an adaptive RCMNN-based control system is designed for the walking control of a biped robot.

Remote control has been frequently used in a lot of auto-matic control systems. Recently, the wireless remote control robots have been developed to dictate a biped robot to move according to the user's commands. The proposed walking command system can be applied to the remote medical robot, the exploration robot, the home security robot, and so on [7]. In the developed biped robot, the Zigbee wireless communication has been designed for the remote communication between the monitoring computer and the robot.

2. Remote Control of the Biped Robot

In order to achieve remote wireless control, a wireless module is used for the communication between the robot and personal computer (PC), as shown in Fig. 1. The wireless module is also used to monitor the motion of the robot. The Zigbee-100, which has 2.4 GHz bandwidth, is designed for robot communication. This peer-to-peer communication module is not easy to be interfered by other equipment or bands.

* Corresponding author. E-mail address: cm1@saturn.yzu.edu.tw

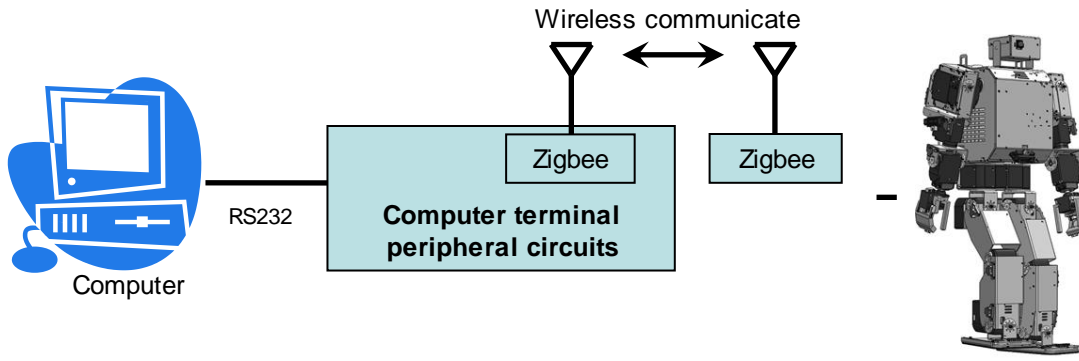


Fig. 1 Block diagram of remote communication robot

3. Adaptive RCMNN-Based Control System

3.1. Cerebellar model neural network

A recurrent CMNN (RCMNN) is introduced as shown in Fig. 2. The basic functions of RCMNN are described as follows.

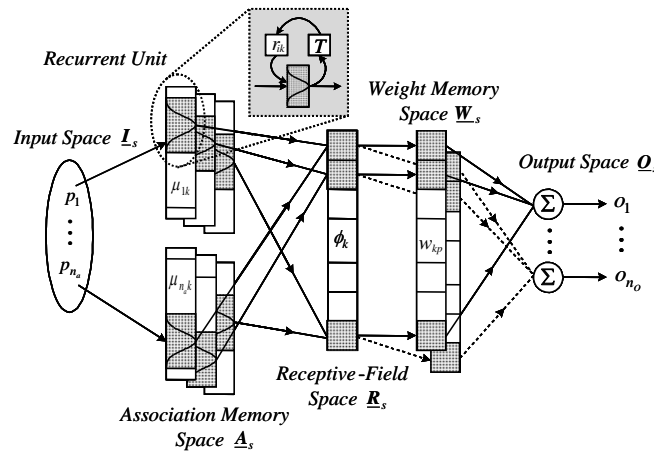


Fig. 2 Architecture of an RCMNN

- (1) *Input space* \underline{I}_s : For a given $\mathbf{p} = [p_1, p_2, \dots, p_{n_a}]^T \in \mathfrak{R}^{n_a}$, where n_a is the number of input state variables, each input state variable p_i is assumed to be quantized into n_e discrete regions (called “neurons”) according to a given control space.
- (2) *Association memory space* \underline{A}_s : Several elements, n_f , can be accumulated as a “block”. In this space, each block performs a receptive-field basis function, and the Gaussian function is adopted here as the receptive-field basis function, which can be represented as

$$\mu_{ik} = \exp \left[\frac{-(p_{rik} - c_{ik})^2}{v_{ik}^2} \right], \text{ for } k = 1, 2, \dots, n_d \quad (1)$$

where μ_{ik} represents the output of the k -th receptive-field basis function for the i -th input with the mean c_{ik} and variance v_{ik} . In addition, the input of this block can be represented as

$$p_{rik}(t) = p_i(t) + r_{ik} \mu_{ik}(t-T) \quad (2)$$

where r_{ik} is the recurrent weight, and $\mu_{ik}(t-T)$ denotes the value of μ_{ik} through delay time T . It is clear that the input of this block contains the memory term $\mu_{ik}(t-T)$, which stores the past information on the network and presents a dynamic mapping.

- (3) *Receptive-field space* \underline{R}_s : The k -th multidimensional receptive-field function is defined as

$$\varphi_k(\mathbf{p}, \mathbf{c}_k, \mathbf{v}_k, \mathbf{r}_k) = \prod_{i=1}^n \mu_{ik} = \exp \left[\sum_{i=1}^n \frac{-(p_{rik} - c_{ik})^2}{v_{ik}^2} \right], \text{ for } k = 1, 2, \dots, n_d \quad (3)$$

where $\mathbf{c}_k = [c_{1k}, c_{2k}, \dots, c_{n_d k}]^T \in \mathfrak{R}^{n_d}$, $\mathbf{v}_k = [v_{1k}, v_{2k}, \dots, v_{n_d k}]^T \in \mathfrak{R}^{n_d}$ and $\mathbf{r}_k = [r_{1k}, r_{2k}, \dots, r_{n_d k}]^T \in \mathfrak{R}^{n_d}$. The multi-dimensional receptive-field functions can be expressed in vector form as

$$\Phi(\mathbf{p}, \mathbf{c}, \mathbf{v}, \mathbf{r}) = [\phi_1, \dots, \phi_k, \dots, \phi_{n_d}]^T \quad (4)$$

where $\mathbf{c} = [\mathbf{c}_1^T, \dots, \mathbf{c}_k^T, \dots, \mathbf{c}_{n_d}^T]^T \in \mathfrak{R}^{n_d n_d}$, $\mathbf{v} = [\mathbf{v}_1^T, \dots, \mathbf{v}_k^T, \dots, \mathbf{v}_{n_d}^T]^T \in \mathfrak{R}^{n_d n_d}$ and $\mathbf{r} = [\mathbf{r}_1^T, \dots, \mathbf{r}_k^T, \dots, \mathbf{r}_{n_d}^T]^T \in \mathfrak{R}^{n_d n_d}$.

(4) *Weight memory space* $\underline{\mathbf{W}}_s$: Each location of $\underline{\mathbf{R}}_s$ to a particular adjustable value in the weight memory space can be expressed as

$$\mathbf{W} = [\mathbf{w}_1, \dots, \mathbf{w}_p, \dots, \mathbf{w}_{n_o}] = \begin{bmatrix} w_{11} & \dots & w_{1p} & \dots & w_{1n_o} \\ \vdots & \ddots & \vdots & \ddots & \vdots \\ w_{k1} & \dots & w_{kp} & \dots & w_{kn_o} \\ \vdots & \vdots & \vdots & \ddots & \vdots \\ w_{n_d 1} & \dots & w_{n_d p} & \dots & w_{n_d n_o} \end{bmatrix} \in \mathfrak{R}^{n_d \times n_o} \quad (5)$$

where $\mathbf{w}_p = [w_{1p}, \dots, w_{kp}, \dots, w_{n_d p}]^T \in \mathfrak{R}^{n_d}$, and w_{kp} denotes the connecting weight value of the p -th output associated with the k -th receptive-field.

(5) *Output space* $\underline{\mathbf{O}}_s$: The output of RCMNN is the algebraic sum of the activated weights in the weight memory and is expressed as

$$o_p = \mathbf{w}_p^T \Phi = \sum_{k=1}^{n_d} w_{kp} \phi_k \quad (6)$$

The outputs of CMNN can be expressed in a vector notation as

$$\mathbf{o} = [o_1, \dots, o_p, \dots, o_{n_o}]^T = \mathbf{W}^T \Phi \quad (7)$$

The architecture of RCMNN is designed to have the advantages of simple structure and dynamic characteristics. The role of the recurrent loops is to consider the past value of the receptive-field basis function in the association memory space. Thus, this RCMNN has dynamic characteristics.

3.2. Adaptive RCMNN-based control system

The biped robot system is highly nonlinear. To effectively control a biped robot, an adaptive RCMNN-based control is introduced in this subsection. The configuration of the proposed adaptive RCMNN control system of the biped robot system is illustrated in Fig. 3. There are two inputs for the adaptive RCMNN controller: first is the tracking error, which is the difference between the reference trajectory d_m and actual trajectory d derived from accelerometer; and second is the angular velocity ω obtained from gyroscope. The output of RCMNN is the control signal U_{Hip} , which adjusts the hip joint to achieve a stable posture. The robot needs this on-line adjusting technique to adjust its original trajectories as it encounters unexpected situations. Another controller is the ZMP compensator, which is also an adaptive RCMNN for auto-tuning the reference trajectories. The two inputs of the ZMP compensator are: the tracking error between the reference ZMP position P_{ZMP}^{ref} and the actual ZMP position P_{ZMP} derived from (8); and the change of this ZMP tracking error. The output of this RCMNN is the ZMP control effort u_{ZMP} . By combining the pre-scheduled walking pattern \mathbf{P} with the output of ZMP compensator u_{ZMP} , and after inverse kinematics, the computed control torque τ_0 can be obtained for the biped robot. By adding the computed torque τ_0 with the hip compensating torque, U_{Hip} , the actual driving torque τ will be applied to drive the biped robot.

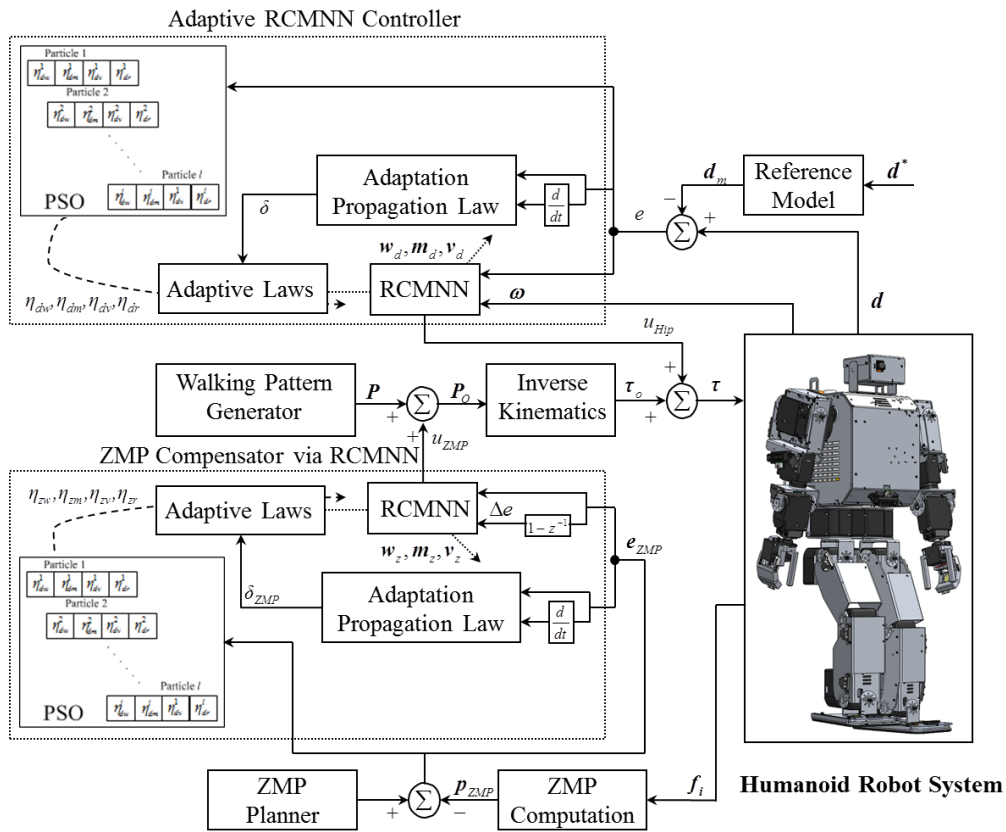
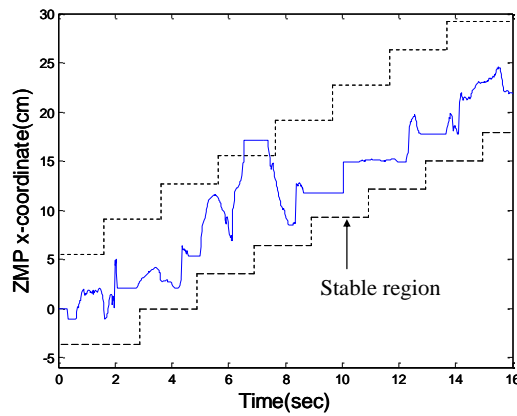
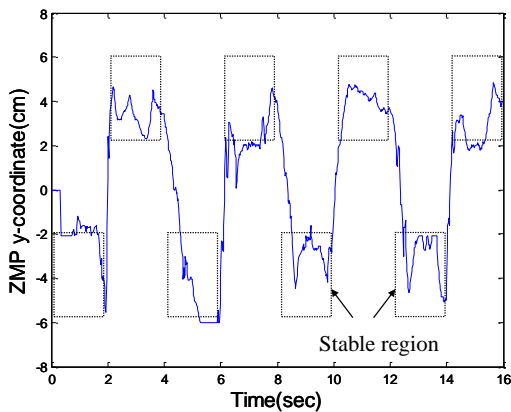


Fig. 3 Block diagram of the adaptive RCMNN control biped robot system

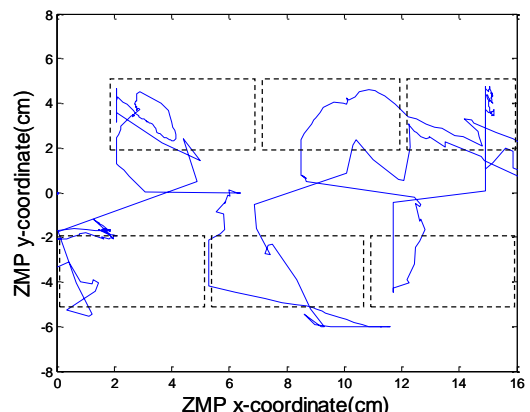
4. Experimental Results



(a) x-direction



(b) y-direction



(c) x-y plane

Fig. 4 Actual ZMP of biped robot

The RCMNN control system is accomplished by the proposed control system, whose structure is depicted in Fig. 2. The RCMNN used here is characterized as $n_e = 9$, $n_f = 4$. The initial learning-rates are selected as $\eta_{zw} = 0.01$ and $\eta_{zn} = \eta_{zv} = \eta_{zr} = 0.001$. The initial values of weights are chosen as $w_{kp} = 0$ and $r_{ik} = 0$. The initial values of parameters of means and variances are chosen as $v_{ik} = 22$ and $[m_{i1}, m_{i2}, m_{i3}, m_{i4}, m_{i5}, m_{i6}, m_{i7}, m_{i8}] = [-49, -35, -21, -7, 7, 21, 35, 49]$ for all i and k . The receptive-fields are selected to cover the input space $\{[-35, 35][-35, 35]\}$ along each input dimension, respectively. These parameters have been chosen through trials to achieve satisfactory control performance. The actual zero moment points (ZMPs) are shown in Fig. 4. The experimental results show that the robot's ZMP has been maintained within a stable region to achieve stable walking.

5. Conclusions

This paper has successfully developed and implemented an intelligent wireless remote control system for a biped robot. The RCMNN-based control system is developed. This adaptive control system has been successfully implemented on a biped robot system. The experimental results demonstrate the ability to achieve satisfactory control performance for stable walking for a high nonlinear biped robot.

Acknowledgement

The support of the Nation Science Council of Republic of China under grant NSC 101-2221-E-155-026-MY3 is gratefully acknowledged.

References

- [1] Y. Sakagami, R. Watanabe, C. Aoyama, S. Matsunaga, N. Higaki, and K. Fujimura, "The intelligent ASIMO: System overview and integration," IEEE/RSJ International Conf. on Intelligent Robots and Systems, September-October 2002, vol. 3, pp. 2478-2483.
- [2] J. H. Kim and J. H. Oh, "Walking control of the humanoid platform KHR-1 based on torque feedback control," Proc. IEEE International Conf. on Robotics and Automation, April-May 2004, vol. 1, pp. 623-628, 2004.
- [3] Y. D. Hong, Y. H. Kim, J. H. Han, J. K. Yoo, and J. H. Kim, "Evolutionary multiobjective footstep planning for humanoid robots," IEEE Transactions on Systems, Man, and Cybernetics, Part C (Applications and Reviews), vol. 41, no. 4, pp. 520-532, July 2011.
- [4] K. Hosoda, T. Takuma, A. Nakamoto, and S. Hayashi, "Biped robot design powered by antagonistic pneumatic actuators for multi-modal locomotion," Robotics and Autonomous Systems, vol. 56, no. 1, pp. 46-53, January 2008.
- [5] Y. S. Cha, K. G. Kim, J. Y. Lee, J. J. Lee, M. J. Choi, M. H. Jeong, et al., "MAHRU-M: A mobile humanoid robot platform based on a dual-network control system and coordinated task execution," Robotics and Autonomous Systems, vol. 59, no. 6, pp. 354-366, June 2011.
- [6] J. S. Albus, "A new approach to manipulator control: The cerebellar model articulation controller (CMAC)," Journal of Dynamic Systems, Measurement and Control, vol. 97, no. 3, pp. 220-227, September 1975.
- [7] T. Kim, E. Kim, and J. W. Kim, "Development of a humanoid walking command system using a wireless haptic controller," International Conference on Control, Automation and Systems, IEEE Press, October 2008, pp. 1178-1183.